Journal of Hazardous Materials 180 (2010) 145–151

Contents lists available at ScienceDirect

Journal of Hazardous Materials

journal homepage: www.elsevier.com/locate/jhazmat

SnO_2-based materials for pesticide degradation

Geoffroy R.P. Malpass[a,*], Douglas W. Miwa[b], Sérgio A.S. Machado[b], Artur J. Motheo[b]

[a] Laboratório de Eletroquímica e Materiais Nanoestruturados, Universidade Federal do ABC, Rua Santa Adélia, 166, Bairro Bangu, Santo André, SP 09.210-170, Brazil
[b] Instituto de Química de São Carlos, Universidade de São Paulo, P.O. Box 780, São Carlos, SP 13560-970, Brazil

ARTICLE INFO

Article history:
Received 12 January 2010
Received in revised form 23 March 2010
Accepted 2 April 2010
Available online 9 April 2010

Keywords:
Photo-assisted electrochemical degradation
Electrochemical degradation
Atrazine
Pesticides

ABSTRACT

This study presents the results of the degradation of the pesticide atrazine using electrochemical and photo-assisted electrochemical degradation techniques using SnO_2-containing electrode of nominal composition electrodes of composition $Ti/Ru_XSn_{1-X}O_2$ (where $X = 0.10$, 0.15, 0.20, 0.25 and 0.30). The materials were characterized *ex situ* and *in situ* in order to correlate the observed atrazine removal rates with electrode morphology/composition. The results obtained demonstrate the effectiveness of the photo-assisted electrochemical degradation. Using purely electrochemical methods the rate of atrazine removal is almost zero at all the electrodes studied. However, the application of photo-assisted degradation results in almost complete atrazine removal in 1 h of electrolysis. The efficiency of atrazine degradation does not seem to be greatly affected by the electrode material or by SnO_2 content, but the overall COD removal is dependent on the SnO_2 content. Overall, the SnO_2-containing electrodes do not reach the level of COD removal (maximum ~21%) seen for the $Ti/Ru_{0.3}Ti_{0.7}O_2$ electrode. An interesting correlation between the morphology factor (φ) and chemical oxygen demand removal is observed.

1. Introduction

In recent years there has been growing interest in the use of electrochemical techniques for the treatment of pollutants [1,2]. Amongst the advantages of using electrochemical methods the most widely quoted are that the catalyst/electrode is immobilized (thus reducing the need to separate the catalyst from the reaction mixture), the variables (i.e. current and potential) are easily controlled and facilitate automation of a process and the cost of the equipment is generally not that high [3].

Electrochemical degradation usually falls into two categories: (1) direct degradation by electron transfer at the electrode surface and (2) indirect degradation through the formation of oxidizing/reducing agents at the electrode which then react with the pollutant in solution [1]. In both these processes the basic factor of interest is the rate of active species produced as a function of to its accessibility for the pollutant species. In many cases direct oxidation is limited by pollutant transfer to the electrode surface and this is generally resolved by reactor design and using porous flow-through electrodes. Indirect degradation is often advantageous as a thermodynamically favorable reaction is employed to generate the active species (e.g. Cl_2 from Cl^-) and higher efficiencies are obtained.

In our laboratory focus has been concentrated on two lines of research. The first is the indirect electrochemical degradation of various polluting substances using oxide electrodes (typically mixtures of RuO_2 and TiO_2) for the *in situ* generation of Cl_2. The matrices investigated include pesticides such as atrazine [4] and carbaryl [5]; real textile waste [6,7] and Cu(II)–humic acid complexes [8]. It was noticed that significant efficiencies are obtained when *in situ* generated chlorine is used. The second approach has been the use of photo-assisted electrochemical degradation (PAEC) which uses the simultaneous application of a UV–vis radiation and of an electrochemical potential, without the generation of Cl_2. The absence of Cl_2 is of interest as chlorinated degradation by-products, formed during chlorination of effluents containing organic species, are suspected carcinogens [9]. Using the PAEC method it is possible to obtain removal efficiencies comparable to using *in situ* Cl_2, depending on the chemical structure of the species and matrix under study. PAEC degradation has been demonstrated to be effective for atrazine [10,11] and dilute dye solutions [12,13], but for carbaryl [14] or for real textile effluent (even in the presence of Cl^-/Cl_2) [14]. However, it is interesting to note that in the case of Alves et al. [15] the phytotoxicity of the textile waste is reduced for the PAEC method when compared to the purely electrochemical method. In this light it is interesting to investigate the effect of using different electrode materials where the interaction of the electrode material and the UV–vis radiation can be improved and the generation of oxidizing species improved.

Atrazine is a widely used triazine herbicide and was chosen as the target molecule for the present study due to the fact that

* Corresponding author. Tel.: +55 11 4437 8430; fax: +55 11 4996 0090.
E-mail addresses: geoffroy.malpass@ufabc.edu.br, geoffmalpass@yahoo.com (G.R.P. Malpass).

0304-3894/$ – see front matter © 2010 Elsevier B.V. All rights reserved.
doi:10.1016/j.jhazmat.2010.04.006

it is used on a wide spectrum of crops, including corn, sorghum, sugar cane, Christmas trees and residential lawns. The activity of atrazine is due to its ability to inhibit photosynthesis in plants [16] and, although it does not present a great risk to human health, in aquatic environments atrazine is highly acutely toxic to aquatic invertebrates. Such factors make it necessary to control the release of atrazine in to the environment and, in fact, the EPAs assessment of atrazine is currently undergoing review [16].

The present study has as its principal aim study the use of alternative electrode materials ($Ti/Ru_XSn_{X-1}O_2$) for the degradation of the pesticide atrazine. The results are compared with those obtained for a commercial DSA® electrode ($Ti/Ru_{0.3}Ti_{0.7}O_2$) and an attempt is made to correlate the data obtained with the morphology of the electrode materials. In previous studies involving the photo-assisted degradation of atrazine it has been our objective to use the TiO_2, added to give mechanical stability to the mixture, present in the electrode matrix as a photocatalyst (albeit in the rutile form) [10,11]. The present study has the same objective, but using SnO_2 (a known photocatalyst [17] in the place of TiO_2.

2. Experimental

2.1. Electrodes and reactor

A single-compartment filter-press cell was used with an oxide electrode plate (exposed geometric area of 14 cm^2), and a Ti-mesh cathode. Two types of electrode were used: a commercial DSA® electrode with nominal composition of $Ti/Ru_{0.3}Ti_{0.7}O_2$ (De Nora, Brazil) and electrodes of composition $Ti/Ru_XSn_{1-X}O_2$ (where $X = 0.10, 0.15, 0.20, 0.25$ and 0.30).

The reactor was mounted by positioning the electrodes between Viton and Teflon® spacers of varying thickness (see Fig. 1). A quartz glass window was placed between the Ti-mesh cathode and the last spacer. The spacers were open in the middle in such a manner that UV–vis radiation was able to pass through both the quartz glass and the Ti-mesh cathode and reach the exposed surface of the electrode. The electrolyte was pumped through the cell by an electric pump at a flow velocity of between 32 and 425 $cm^3\ min^{-1}$, depending on the experiment to be performed. The UV radiation was provided by a 250 W high-pressure mercury lamp (Philips) with a fluency rate of 0.417 W cm^{-2} (at $\lambda = 254$ nm). The distance between the lamp and the electrode was 7 cm, and the fluency rate of the light incident on the DSA® electrode (after passing through the quartz glass and counter electrode) was 0.113 W cm^{-2}. The entire setup was placed in a closed box, which was equipped with an exhaust fan to dissipate the heat produced by the UV radiation source. A membrane (IONAC), which was open in the same manner as the spacers, with a strip that was positioned in an electrolyte bath, was not used to separate the cell compartments but to provide an *in situ* probe connected to the reference electrode. The connection between the membrane walls, which was in contact with the working solution inside the cell, and the reference electrode was made by a membrane strip in contact with a bath of concentrated sodium sulfate (Fig. 2). The reference electrode was a reversible hydrogen electrode (RHE). The reference electrode was necessary to perform the cyclic voltammetric experiments, and it was also interesting to monitor the potential of the working electrode during galvanostatic treatment, as this is a convenient way to monitor any poisoning or corrosion of the electrode surface (i.e. increase in potential).

For analysis of the morphology factor a single-compartment electrochemical cell was employed with the working electrodes described above, but with an active area exposed to the solution of 1.56 cm^2. For the experimental setup the reader is directed to [18,19].

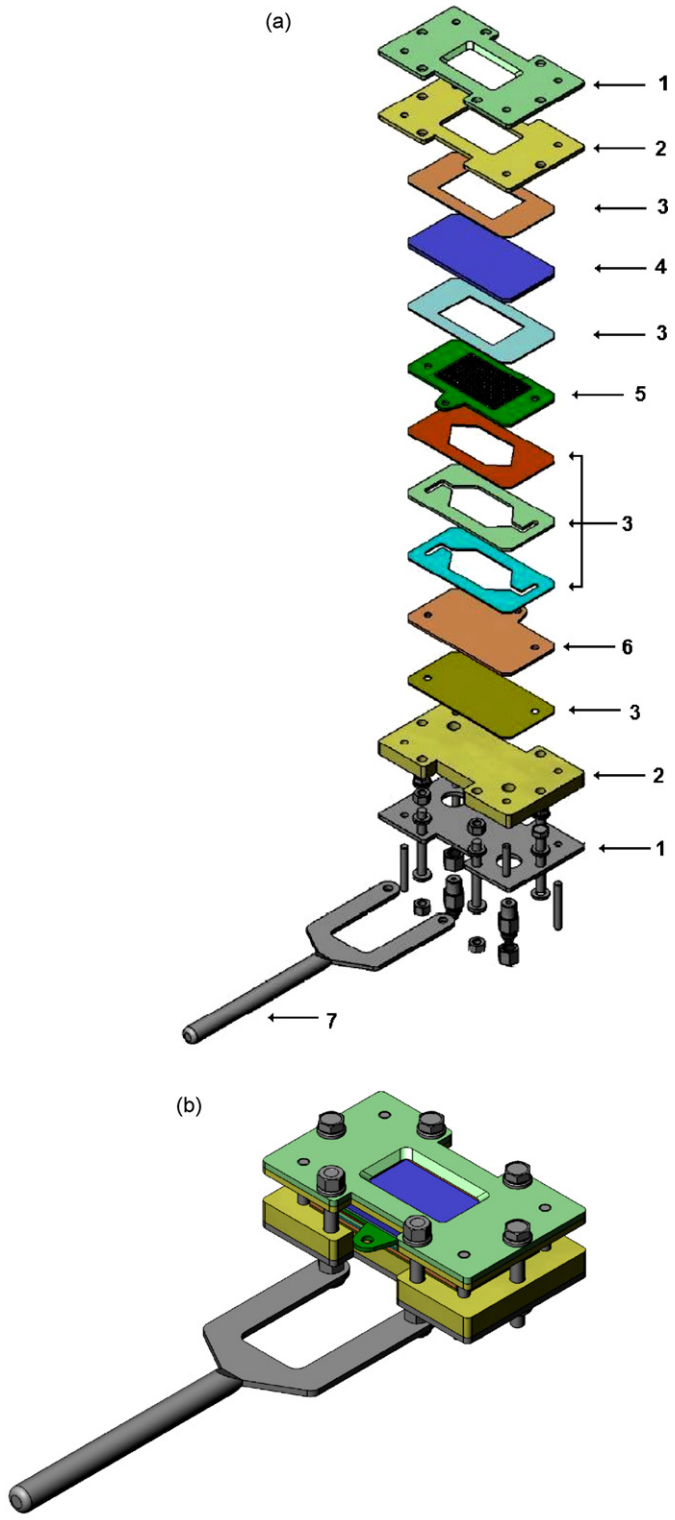

Fig. 1. Electrochemical flow-cell used in study (A) exploded view where (1) outer steel plate with connecting nuts and bolts; (2) Teflon® plate; (3) Viton® spacers; (4) quartz glass plate; (5) Ti-mesh counter electrode; (6) working electrode ($Ti/Ru_{0.3}Ti_{0.7}O_2$ or $Ti/Ru_XSn_{1-X}O_2$—area exposed to the electrolyte: 14 cm^2), and (7) support. (B) Mounted view of cell.

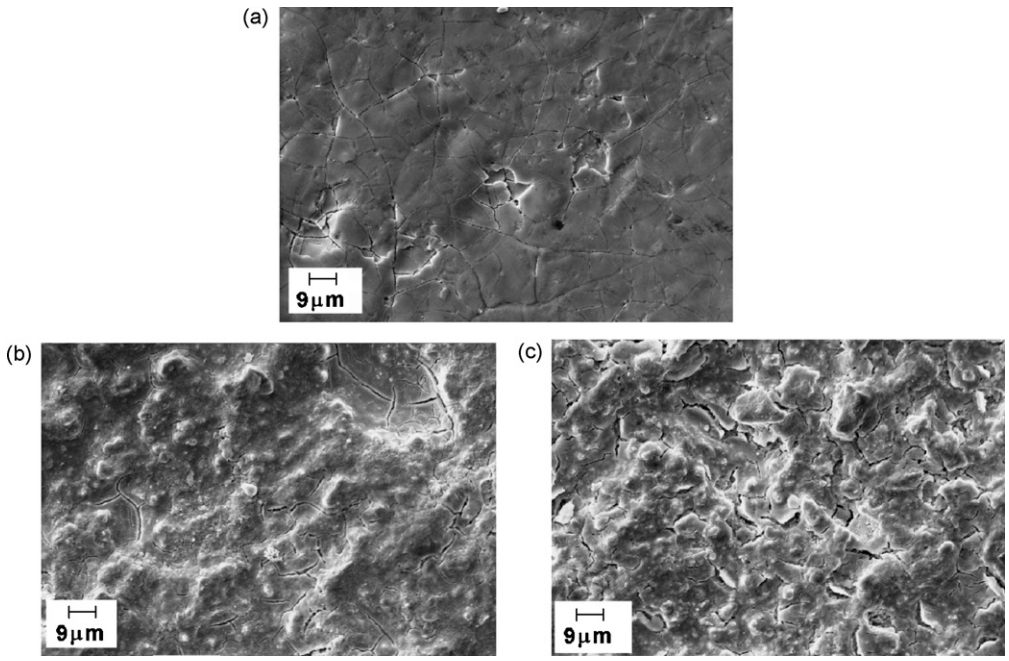

Fig. 2. SEM images of the SnO_2-containing electrodes ($Ti/Ru_XSn_{1-X}O_2$): (a) $Ti/Ru_{0.3}Sn_{0.7}O_2$; (b) $Ti/Ru_{0.2}Sn_{0.8}O_2$; (c) $Ti/Ru_{0.1}Sn_{0.9}O_2$. Magnification: 2500×.

2.2. Electrode preparation

The $Ti/Ru_XSn_{1-X}O_2$ electrodes were prepared in the laboratory by the standard technique of thermal decomposition of the appropriate mixtures of precursor salts (0.2 mol dm^{-3} $SnCl_2$ and $RuCl_3 \cdot nH_2O$) dissolved in 1:1 HCl (v/v) [20]. The mixture was applied uniformly painted onto the previously degreased (isopropyl alcohol followed by ultrasound for 10 min) and etched (in boiling oxalic acid for 30 min) Ti plate (thickness 1 mm). After each addition of the precursors, the solvent was initially removed by passing hot air and then the electrode was calcinated at 400 °C for 10 min and subsequently weighed. The calcination of the electrodes was performed at 400 °C under a flux of oxygen (5 cm^3 min^{-1}). When the desired mass was achieved the electrode was calcinated further at 400 °C for an hour. Each electrode was projected to have an oxide thickness of ~2 μm.

The electrode of nominal composition $Ti/Ru_{0.3}Ti_{0.7}O_2$ was obtained commercially from De Nora, Brazil.

2.3. Materials and equipment

All electrochemical measurements were performed using a potentiostat/galvanostat (Autolab, model SPGSTAT). The analysis of the atrazine concentration was performed by high-performance liquid chromatography (Shimadzu, model LC-10AD VP), and samples of the electrolyte solution were obtained at predetermined time intervals during the degradation process. The supporting electrolyte (Na_2SO_4) was obtained from Merck and used without purification. Atrazine was obtained as a standard (Riedal Haan) and used without further purification.

2.4. Experimental procedure

For the each electrode the voltammetric profile was stabilized by performing 100 sweeps at 50 mV s^{-1}, in the potential range under study, before each cyclic voltammetry measurement. After this procedure, all the CVs presented in this study represent the 3rd sweep. Our preliminary studies showed that the VC was unaltered after the 2nd sweep at the sweep rate used.

Three different degradation techniques were employed as follows: (a) photocatalytic (interaction of UV radiation and electrode surface), (b) electrochemical (EC—application of a constant current), and (c) photo-assisted electrochemical (PAEC—simultaneous application of a constant current and UV radiation). All electrolyses were performed using a solution volume of 0.25 L of 0.033 mol dm^{-3} Na_2SO_4 + 20 mg dm^{-3} atrazine, at a flow rate of 425 cm^3 min^{-1} and a current density of 10 mA cm^{-2}. The value of 10 mA cm^{-2} was used as it was the most efficient used in a previous study performed in this laboratory [10] and is used so as to provide a comparison with previous work. Any deviation from this procedure is reported at the appropriate point in the text.

3. Results

3.1. Ex situ analysis

Ex situ analysis of the synthesized materials was performed using Scanning Electron Microscopy (SEM) and Fig. 2 presents examples of the micrographs obtained for a selection of the materials understudy. As can be observed from Fig. 2 all the materials present the typical "cracked mud" morphology of electrode produced by thermal decomposition [21]. This kind of morphology can be attributed to the occurrence of thermal shocks that occur at the high temperatures [21] and it should be noted that the structure tends to become less compact as the SnO_2 content is increased.

Analysis of the chemical composition of the electrodes by EDX indicated that there was an enrichment of the film by RuO_2 (SnO_2 depletion) during the preparation procedure. Fig. 3 presents the level of enrichment for the synthesized materials compared to the theoretical levels in the original precursor mixture. This enrichment is in agreement with previous studies presented in the literature [20,22] and can be explained by the fact that previous authors have noted that $SnCl_4$ is volatilized during the calcination step [20].

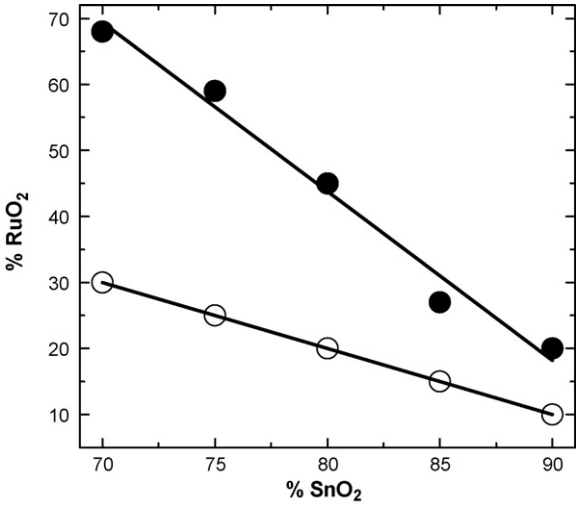

Fig. 3. Variation of the % of RuO_2 for electrodes of nominal composition $Ti/Ru_XSn_{1-X}O_2$: (○) theoretical composition, and (●) real composition.

3.2. *In situ analysis*

In the present study the *in situ* analysis was performed by the technique of cyclic voltammetry and by determination of the morphology factor (φ) [18,19].

3.2.1. *Cyclic voltammetry*

Fig. 4 presents the cyclic voltammograms (CV) of the electrodes under study and the inset presents the anodic charges associated with each electrode. The electrodes present the typical characteristics of this kind of material: between the potential limits of 0.4–1.4 V, the voltammogram is featureless; at potentials above this, the oxygen evolution reaction (OER), which is characterized by a rapid increase in the current, occurs. In accordance with the voltammograms (Fig. 4) the greater anodic charge can be observed for electrodes that contain the greater quantity of RuO_2.

3.2.2. *Morphology factor*

The morphology factor (φ) can be considered a measure of the contribution of the internal sites of the electrode to the overall

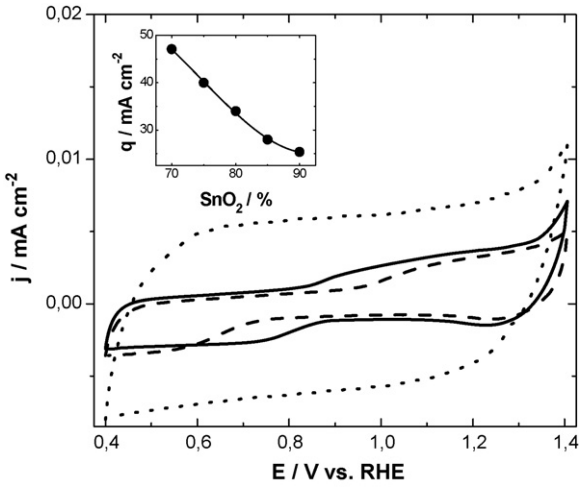

Fig. 4. Voltammetric profiles (3rd sweep) of (dotted line) $Ti/Ru_{0.3}Sn_{0.7}O_2$;(solid line) $Ti/Ru_{0.2}Sn_{0.8}O_2$; (dashed line) $Ti/Ru_{0.1}Sn_{0.9}O_2$. Supporting electrolyte: H_2SO_4 (0.5 mol L^{-1}). Sweep rate: 50 mV s^{-1}. Area exposed to the electrolyte: 14 cm^2. *Inset*: Anodic charges as a function of the SnO_2 content.

Table 1
Values of the morphology factor (φ) for the electrodes used in this study.

Electrode	φ (C_{dT}/C_{di})
$Ti/Ru_{0.3}Sn_{0.7}O_2$	0.24
$Ti/Ru_{0.25}Sn_{0.75}O_2$	0.30
$Ti/Ru_{0.2}Sn_{0.8}O_2$	0.37
$Ti/Ru_{0.15}Sn_{0.85}O_2$	0.50
$Ti/Ru_{0.1}Sn_{0.9}O_2$	0.52

differential capacitance [19]:

$$\varphi_{\text{Morph}} = \frac{C_i}{C_T} \quad (1)$$

where C_i and C_T are, respectively, the "internal" and "total" differential capacitances of the film and they represent the corresponding surface areas. The value of φ was determined for the electrodes used in this study according to the method detailed by in [18,19] and readers are directed to these references for complete details of the process.

In accordance with Eq. (1), the value of φ can vary between 0 and 1. When it tends to 0 the internal sites of the electrode have a small or negligible influence on the overall differential capacitance. On the other hand, values of φ approaching 1 indicate an electrode structure with a large internal region. The value of φ was obtained by performing 20 consecutive voltammetric curves at several potential sweep rates (5–300 mV s^{-1}) covering a 0.1 or 0.2 V capacitive potential, depending on the electrode under study. For the $Ti/Ru_{0.3}Ti_{0.7}O_2$ electrode the potential limits were 0.435–0.535 V. For the SnO_2 electrodes the limits were in the region of 0.365–0.465 V.

Table 1 presents the values of the morphology factor for the electrodes under study and as the SnO_2 content increases the value of φ increases considerably, indicating that the internal area increases with SnO_2 addition. A value of 0.52 is obtained for the $Ti/Ru_{0.3}Sn_{0.7}O_2$ electrode and this compares well with results obtained for a commercial $Ti/Ru_{0.3}Ti_{0.7}O_2$ DSA® sample (0.49 [18]), but is greater than that of a lab-made $Ti/Ru_{0.3}Ti_{0.7}O_2$ sample (0.22 [18]). This is in agreement with the micrographs in Fig. 2 where there is an opening of the structure as the SnO_2 content increases.

3.2.3. *Cyclic voltammetry: presence of atrazine and UV–vis irradiation*

Fig. 5 presents the cyclic voltammograms for the same electrodes given in Fig. 3, but this time in a flow-cell and with the positive potential limits extended to encompass the region of the oxygen evolution reaction, which is the region where organic oxidation is purported to occur [23].

In the pure electrolyte, with no light application, the electrodes again present the typical characteristics of this kind of materials between the potential limits of 0.4–1.4 V, the voltammogram is featureless; at potentials above this, the oxygen evolution reaction, which is characterized by a rapid increase in the current, occurs. When simultaneous UV–vis radiation is applied, it can be observed that the potential associated with the OER is substantially reduced. This is a significant result, as the intermediates involved in the formation of O_2 are considered responsible for oxidation at oxide electrodes [23], and any reduction in the potential of the formation of such intermediates represents a considerable energy saving.

The results are best described by the model presented by Comninellis [23], where so-called active electrodes (e.g. RuO_2) promote oxidation via formation of higher oxides (MO_{X+1}) and non-active electrodes (e.g. SnO_2) promote oxidation through the formation of adsorbed hydroxyl radicals ($MO_X(^{\bullet}OH)$). Both (MO_{X+1}) and ($MO_X(^{\bullet}OH)$) are also intermediates in the formation of O_2 and

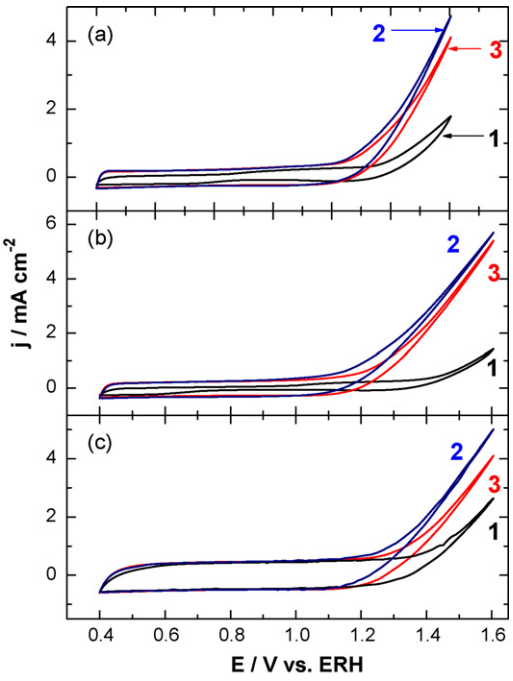

Fig. 5. Cyclic voltammograms (3rd sweep) of electrodes of nominal composition $Ti/Ru_XSn_{1-X}O_2$ in: (curve 1) 0.033 mol L^{-1} Na_2SO_4; (curve 2) 0.033 mol L^{-1} $Na_2SO_4 + h\nu$; and (curve 3) 0.033 mol L^{-1} Na_2SO_4 + 20 mg L^{-1} atrazine + $h\nu$. (a) $Ti/Ru_{0.3}Sn_{0.7}O_2$; (b) $Ti/Ru_{0.2}Sn_{0.8}O_2$; (c) $Ti/Ru_{0.1}Sn_{0.9}O_2$. Sweep rate = 50 mV s^{-1}. Area exposed to the electrolyte: 14 cm^2.

as a result organic oxidation occurs in potential regions where O_2 evolution also occurs.

When atrazine is added to the electrolyte, it can be observed that the potential of the OER undergoes an increase (reduction in the current density) in the presence of UV–vis radiation. This fact indicates that atrazine ($\lambda_{max} \sim 221$ nm) absorbs a certain amount of radiation before it reaches the electrode surface. This might indicate that the direct photolysis of atrazine in solution is a possible degradation pathway [24].

3.3. Degradation studies

3.3.1. Atrazine removal

As stated in the experimental section the materials under study in the paper were tested for their activity in organic oxidation. The pesticide atrazine was chosen as the target molecule as it has been widely studied for a number of called advanced oxidation studies (AOPs) and also in this laboratory in electrochemical [4] and photo-assisted treatment systems [10]. The degradation studies were performed under galvanostatic conditions with the aim of being able to compare with previous studies in this laboratory [10]. The current density chosen was 10 mA cm^{-2} as this value was used previously [10] and was shown to be the best for a commercial $Ti/Ru_{0.3}Ti_{0.7}O_2$ DSA® sample.

In Fig. 6a, a chromatogram of the atrazine peak is given, before degradation and after both electrochemical and photo-assisted electrochemical degradation for 30 min. It can be observed, in agreement with previous studies [4,10], that the purely electrochemical removal of atrazine is limited and that the extent of atrazine removal after 30 min is much greater when the photo-assisted method is applied.

Fig. 6b presents the concentration–time profile for the degradation of atrazine at 10 mA cm^{-2} in the presence and the absence of UV–vis radiation for the $Ti/Ru_{0.3}Sn_{0.7}O_2$ electrode. From Fig. 6b it can be seen that the rate of removal of the combined method (PAEC) is much more accentuated than for the purely electrochemical method, in agreement with previous results [10]. In approximately 60 min >99% of the atrazine present in solution is removed using the PAEC method at the $Ti/Ru_{0.3}Ti_{0.7}O_2$ electrode. If the theoretical combination of the photochemical and electrochemical techniques (solid line, Fig. 6) is taken into consideration, it can be verified that the PAEC method is much more effective than the mere sum of its parts. These results are in accordance with previously published results for a $Ti/Ru_{0.3}Ti_{0.7}O_2$ commercial DSA® material [10], demonstrating the repeatability of the results. There is no significant difference in the extent or rate of removal for the different electrodes studied during the PAEC degradation. In all cases the removal of atrazine presents pseudo 1st order kinetics (Fig. 7), again in agreement with previous studies [10]. The value of the rate constant does not vary significantly for the different materials, being in the region of $0.6/7 \times 10^{-3}$ s^{-1} when the photo-assisted method is applied, again in agreement with values previously obtained previous studies from this laboratory [10].

There are probably two main reasons for the increase in the rate of atrazine removal using the PAEC system: (1) involvement of the electrochemically inert TiO_2 in the photo-catalytic process and (2) separation of the electron-hole pair generated in (1) by application of an external electric potential, which is known to increase the degradation efficiency [25].

It is interesting to note that the use of "non-active" materials (i.e. SnO_2) does not result in an increase in the rate of degrada-

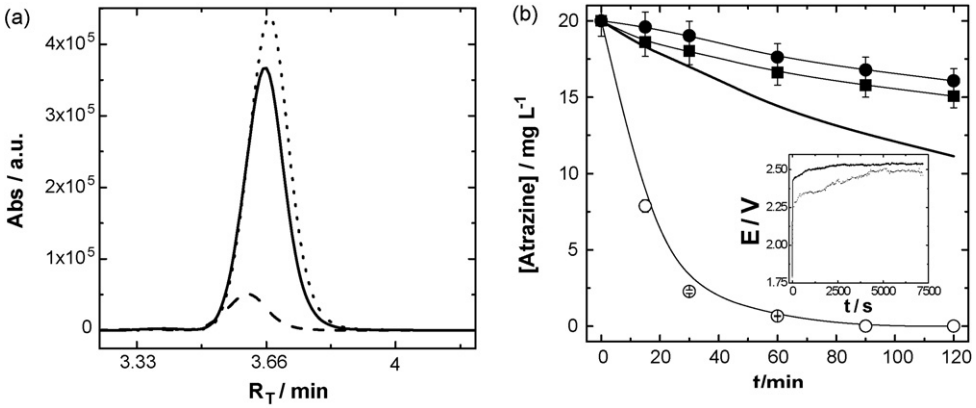

Fig. 6. (a) Chromatogram representing the peak of atrazine: (dotted line) before degradation; (solid line) after 30 min of EC degradation and (dashed line) after 30 min of PAEC degradation. Electrode: $Ti/Ru_{0.3}Sn_{0.7}O_2$. j = 10 mA cm^{-2}. (b) Time concentration-profile for Atrazine degradation at a $Ti/Ru_{0.3}Sn_{0.7}O_2$ electrode at 10 mA cm^{-2}: (●) EC; (○) PAEC; (■) PC (*photocatalysis*). Solid line represents theoretical value of PC + EC.

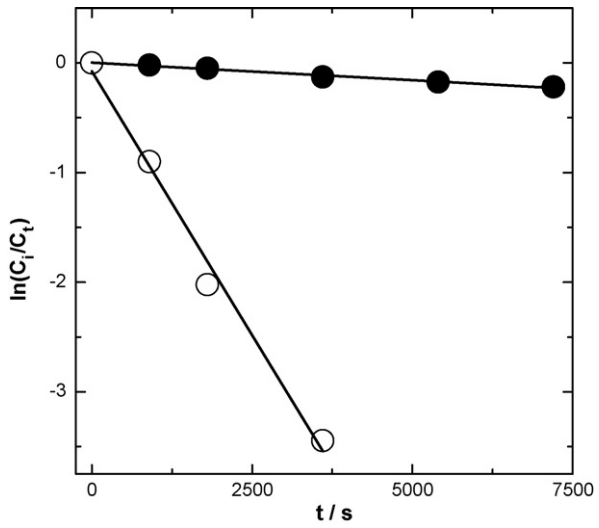

Fig. 7. Pseudo 1st order plot for (○) PAEC and (●) EC degradation at 10 mA cm^{-2}; for the Ti/$Ru_{0.3}Sn_{0.7}O_2$ electrode in 0.033 mol L^{-1} Na_2SO_4 + 20 mg L^{-1} atrazina.

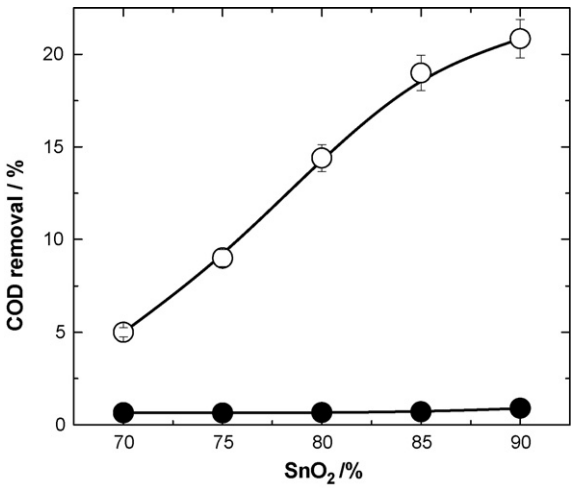

Fig. 9. Removal of COD as a function of SnO_2 content (%) for (●) EC and (○) PAEC degradation at 10 mA cm^{-2}. Electrolysis time: 120 min.

tion compared to the "active" electrode. This is probably due to the fact that atrazine is extremely difficult to degrade and that there is little evidence of an adsorption process occurring (when the voltammograms in Fig. 5 are considered).

For any prospective treatment process the extent of the electrical energy spent to oxidize/reduce a given species is of extreme importance. In many so-called *Advanced Oxidation Processes* the removal of a given pollutant follows pseudo 1st order kinetics and the *Electrical Energy per Order* (E_{EO}/kWh order^{-1}) can be applied [26]. In the current study, the electrical energy per order for a batch process can be applied as

$$E_{EO} = \frac{(P_{el})(t)}{(V)(\log(c_i/c_f)} \quad (2)$$

where P_{el} is the electrical power input in kW, t is the time in h, V is the solution volume in m^3, and c_i and c_f are the initial and final concentrations, respectively, of the substance of interest. The use of Eq. (1) implicitly implies 1st order kinetics.

Fig. 8 presents the variation of the E_{EO} as a function of the SnO_2 content of the electrode. One very interesting point is the fact that for the purely electrochemical system the efficiency increases with increasing SnO_2 content, which can probably be attributed to the non-active nature of this material, according to the mechanism proposed by Comninellis [23]. The non-active nature of SnO_2 would promote the formation of hydroxyl radicals (HO•) which promote less selective, but more rapid, degradation. When the combined method is used, there is little difference in the energy consumed between the electrodes. Although there is an increase in the E_{EO} value as the SnO_2 content increases, this is probably due to the resistivity of the material, which increases as the SnO_2 also increases and thus increases the consumption (Eq. (1)). The lowest E_{EO} value obtained is for the Ti/$Ru_{0.3}Sn_{0.7}O_2$ material at 0.64 kWh m^{-3} order^{-1}, which is lower than that obtained for Ti/$Ru_{0.3}Ti_{0.7}O_2$ commercial DSA® material (0.79 [10]).

In Brazil, electricity (kWh) is presently sold at R$ 0.30/kWh [27] (Brazilian reals). As the Brazilian real currently translates to approximately US$ 1 = R$ 1.80, 1 kWh would cost US$ 0.17. The lowest E_{EO} value obtained is for the Ti/$Ru_{0.3}Sn_{0.7}O_2$ material at 0.64 kWh m^{-3} order^{-1}, which is lower than that obtained for Ti/$Ru_{0.3}Ti_{0.7}O_2$ commercial DSA® material (0.79). This would result in a price of US$ 0.11 m^{-3} order^{-1} or US$ 0.11 to reduce the atrazine present in 1 m^3 by one order of magnitude.

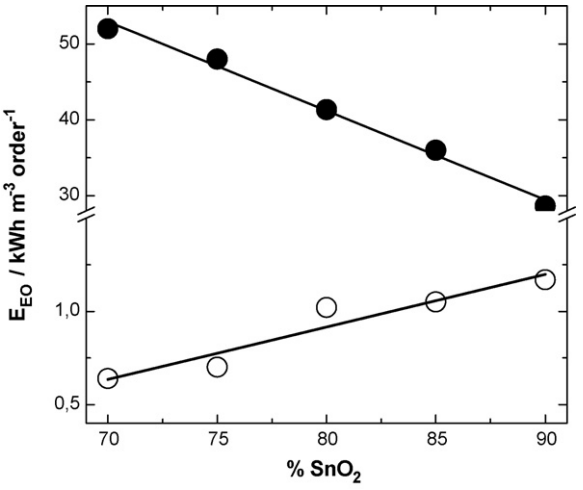

Fig. 8. Variation of the E_{EO} as a function of SnO_2 content (%) for (●) EC and (○) PAEC degradation at 10 mA cm^{-2}.

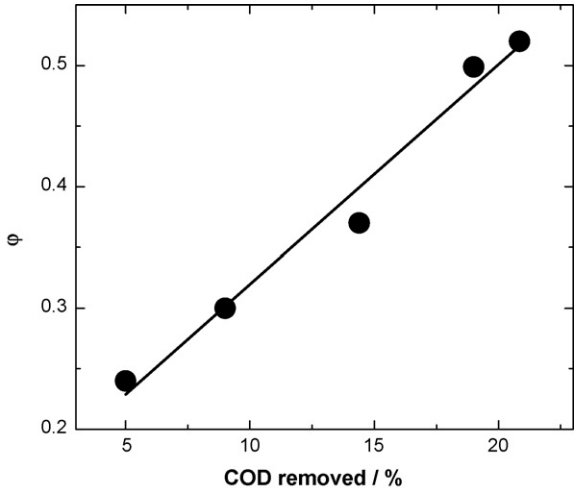

Fig. 10. Correlation between the morphology factor and the amount of COD removed during PAEC degradation at 10 mA cm^{-2}.

3.3.2. COD removal

A fundamental aspect of any prospective treatment system is the ability to remove organic load. In the present study is this parameter was investigated by determining the level of Chemical Oxygen Demand (COD) before and after the degradation. Fig. 9 presents the level of COD removal for the electrodes under study. It is possible to identify that the extent of COD removal is greater as the SnO_2 content increases and reaches a maximum of ~21% for the $Ti/Ru_{0.1}Sn_{0.9}O_2$ after 120 min. However, it should be noted that the level of COD removal is much less than for the $Ti/Ru_{0.3}Ti_{0.7}O_2$ commercial DSA® material (~79% removal [10]).

An interesting linear correlation of the extent of COD removal with the morphology factor can be seen in Fig. 10. This indicates that the internal area of the electrode plays a part in the degradation of atrazine by-products. Such a correlation is not possible for the purely electrochemical degradation method as the values are extremely low.

4. Conclusions

The results obtained demonstrate the effectiveness of the photo-assisted electrochemical degradation of organic molecules. The efficiency of atrazine degradation does not seem to be greatly affected by the electrode material or by SnO_2 content, but the overall COD removal is dependent on the SnO_2 content. Overall, the SnO_2-containing electrodes do not reach the level of COD removal seen for the $Ti/Ru_{0.3}Ti_{0.7}O_2$ materials.

Previous studies in this laboratory have shown that atrazine is extremely difficult to degrade by purely electrochemical methods or without the formation of a strong oxidizing agent. In this light it is interesting to suggest that the increased level of COD removal is probably due to the formation of smaller degradation products that can then migrate to the inner sites and undergo further degradation. The fact that SnO_2 is also more effective at producing strong oxidizing agents would then result in a more rapid rate of COD removal:

$$\text{Atrazine} \overset{\text{Surface PAEC}}{\longrightarrow} \text{Smaller Species} \overset{\text{internal EC}}{\longrightarrow} CO_2$$

Acknowledgements

The authors would like to thank FAPESP (Brazil) for the funding provided.

References

[1] C.A. Martinez-Huitle, E. Brillas, Decontamination of wastewaters containing synthetic organic dyes by electrochemical methods: a general review, Appl. Catal. B 87 (2009) 105–145.
[2] C.A. Martinez-Huitle, S. Ferro, Electrochemical oxidation of organic pollutants for the wastewater treatment: direct and indirect processes, Chem. Soc. Rev. 35 (2006) 1324–1340.
[3] K. Juttner, U. Galla, H. Schmieder, Electrochemical approaches to environmental problems in the process industry, Electrochim. Acta 45 (2000) 2575–2594.
[4] G.R.P. Malpass, D.W. Miwa, S.A.S. Machado, A.J. Motheo, Oxidation of the pesticide atrazine at DSA® electrodes, J. Hazard. Mater. 137 (2006) 565–572.
[5] D.W. Miwa, G.R.P. Malpass, S.A.S. Machado, A.J. Motheo, Electrochemical degradation of carbaryl on oxide electrodes, Water Res. 40 (2006) 3281–3289.
[6] G.R.P. Malpass, D.W. Miwa, D.A. Mortari, S.A.S. Machado, A.J. Motheo, Decolorisation of real textile waste using electrochemical techniques: effect of the chloride concentration, Water Res. 41 (2007) 2969–2977.
[7] G.R.P. Malpass, D.W. Miwa, D.A. Mortari, S.A.S. Machado, A.J. Motheo, Decolorisation of real textile waste using electrochemical techniques: effect of electrode material, J. Hazard. Mater. 156 (2008) 170–177.
[8] C.P. Barbosa, G.R.P. Malpass, D.W. Miwa, L. Gomes, R. Bertazzoli, A.J. Motheo, Electrochemical removal of Cu^{II} in the presence of humic acid, J. Braz. Chem. Soc. 21 (2010) 651–658.
[9] K. Gopal, S.S. Tripathy, J.L. Bersillon, S.P. Dubey, Chlorination byproducts, their toxicodynamics and removal from drinking water, J. Hazard. Mater. 140 (2007) 1–6.
[10] G.R.P. Malpass, D.W. Miwa, A.C.P. Miwa, S.A.S. Machado, A.J. Motheo, Photo-assisted electrochemical oxidation of atrazine on a commercial $Ti/Ru_{0.3}Ti_{0.7}O_2$ DSA® electrode, Environ. Sci. Technol. 41 (2007) 7120–7125.
[11] G.R.P. Malpass, D.W. Miwa, L. Gomes, E.B. Azevedo, W.F. Vilela, M.T. Fukunaga, J.R. Guimarães, R. Bertazzoli, S.A.S. Machado, A.J. Motheo, Photo-assisted electrochemical degradation of the commercial herbicide atrazine, Water Science and Technology, in press.
[12] M. Catanho, G.R.P. Malpass, A.J. Motheo, Photoelectrochemical treatment of the dye reactive red 198 using DSA® electrodes, Appl. Catal. B-Environ 62 (2006) 193–200.
[13] M. Catanho, G.R.P. Malpass, A.J. Motheo, Evaluation of electrochemical and photoelectrochemical methods for the degradation of three textile dyes, Quim. Nova 29 (2006) 983–989.
[14] G.R.P. Malpass, D.W. Miwa, A.C.P. Miwa, S.A.S. Machado, A.J. Motheo, Study of photo-assisted electrochemical degradation of carbaryl at dimensionally stable anodes DSA®, J. Hazard. Mater. 167 (2009) 224–229.
[15] P.A. Alves, G.R.P. Malpass, D.W. Miwa, A.J. Motheo, Photo-assisted electrochemical degradation of real textile wastewater, Water Sci. Technol. 61 (2010) 491–498.
[16] Atrazine Science Reevaluation: Potential Health Impacts (SAP docket), USEPA, www.regulations.gov/search/Regs/home.html#docketDetail?R=EPA-HQ-OPP-2009-0759 (viewed March 15/03/2010).
[17] A. Mills, R.H. Davies, D. Worsley, Water-purification by semiconductor photocatalysis, Chem. Soc. Rev. 22 (1993) 417–425.
[18] L.M. Da Silva, L.A. De Faria, J.F.C. Boodts, Determination of the morphology factor of oxide layers, Electrochim. Acta 47 (2001) 395–403.
[19] G.R.P. Malpass, R.S. Neves, A.J. Motheo, A comparative study of commercial and laboratory-made $Ti/Ru_{0.3}Ti_{0.7}O_2$ DSA® electrodes: "In situ" and "ex situ" surface characterisation and organic oxidation, Electrochim. Acta 52 (2006) 936–944.
[20] T.A.F. Lassali, L.M.C. Abeid, L.O.S. Bulhões, J.F.C. Boodts, Surface characterization of thermally prepared, Ti-supported, Ir-based electrocatalysts containing Ti and Sn, J. Electrochem. Soc. 144 (1997) 3348–3354.
[21] S. Trasatti, Physical electrochemistry of ceramic oxides, Electrochim. Acta 36 (1991) 225–231.
[22] R. Berenguer, C. Quijada, E. Morallón, Electrochemical characterization of SnO_2 electrodes doped with Ru and Pt, Electrochim. Acta 54 (2009) 5230–5238.
[23] C. Comninellis, Electrocatalysis in the electrochemical conversion/combustion of organic pollutants for waste-water treatment, Electrochim. Acta 39 (1994) 1857.
[24] H.D. Burrows, M. Canle, J.A. Santaballa, S. Steenken, Reaction pathways and mechanisms of photodegradation of pesticides, J. Photochem. Photobiol. B 67 (2002) 71.
[25] K. Vinodgopal, P.V. Kamat, Combine electrochemistry with photocatalysis, CHEMTECH 26 (1996) 18–22.
[26] J.R. Bolton, K.G. Bircher, W. Tumas, C.A. Tolman, Figures-of-merit for the technical development and application of advanced oxidation technologies for both electric – and solar-driven systems – (IUPAC Technical Report), Pure Appl. Chem. 73 (2001) 627–637.
[27] Agencia Nacional de Energia Elétrica (ANEEL), Agency of the Brazilian Ministry of Mines and Energy, http://aneel.gov.br/ (accessed 20/03/2010).